PAPER 34 (SESSION III)

A fractographic study of the stress corrosion cracking of titanium and its alloys

D. T. POWELL and J. C. SCULLY,
University of Leeds, England.

Summary

The stress corrosion cracking of titanium (99·2% purity) and Ti-5%Al-2·5%Sn alloy has been studied in two environments: methanol containing 1·5 wt.% HCl (1·06 wt.% water) and aqueous chloride solutions with chloride ion concentrations from 0·1 ppm (distilled water) to 18,000 ppm (3%NaCl).

Two types of test were employed: (i) U-bend tests, and (ii) dynamic straining in contact with the environment on an Instron Tensile Testing Machine. The fracture surfaces of the specimens were examined using a scanning electron microscope.

Fracture surfaces of the Ti-5%Al-2·5%Sn alloy exhibited interrupted transgranular cleavage, with clearly defined river patterns, in both types of test. For the Instron tests, cracking in 3%NaCl was produced by strain rates from 0·05 cm/min to 0·2 cm/min. Cracking was indicated by failure without necking very close to the U.T.S. with a considerable reduction in the total strain to fracture, a single crack occurring perpendicular to the tensile axis. The crack velocity was found to increase as the chloride ion concentration was raised. The velocity was 1·5 mm/min in distilled water and 11 mm/min in 3% NaCl.

U-bend fracture surfaces of the metal broken in the methanolic environment exhibited intergranular separation, but cracking of this material did not occur in the dynamic tests.

Both materials also suffered a slow form of attack on grain boundaries in the methanolic solution. When subsequently broken in air, the specimens exhibited featureless intergranular fracture surfaces. Residual stresses were found to accelerate this process. Transmission electron micrographs are shown to illustrate attack on grain boundaries in thin foils. A proposed mechanism of slow strain-rate hydrogen embrittlement will be briefly discussed.

Introduction

The effects of environment upon the fracture of titanium alloys have been known for some time. Both liquid metal embrittlement [1] and fuming nitric acid [2] were found to cause premature failure. It was only in 1965, however, that Brown [3] reported that titanium alloys suffered a lowering of resistance to crack propagation in 3% aqueous NaCl solution. The practical consequences of this latter phenomenon, which may curtail the employment of titanium alloys in marine environments, are considerable and much effort has been made (a) to evaluate and characterize the kinetics of cracking in many different alloys with reference to such variables as heat treatment temperature and quenching rate, and (b) to establish the mechanism of cracking.

Linear elastic fracture mechanics has been applied and many of the screening tests have used a pre-cracked notch bar test sample of large

enough dimensions to establish plane strain conditions at the crack tip. Such tests have shown that in addition to aqueous chloride solutions, many organic compounds such as methanol, benzene and pentane can cause failure.

The characteristics of cracking in aqueous chloride environments are:

(i) a wide range of crack propagation rates, depending upon the alloy composition, the heat treatment employed and the concentration of the chloride ion. Rates as high as 1 in/min have been reported 4 .

(ii) a diminished succeptibility to cracking as β-stabilizing elements are added, e.g. Mo, V etc. [5].

(iii) crack velocity dependence upon potential. Beck [6] found that the average velocity of crack propagation during stress corrosion is linearly related to potential in chloride, bromide and iodide solutions and that for a Ti-8Al-1Mo-1V alloy, cracking occurs at potentials more positive than −1000 mV to a saturated calomel electrode.

In this paper, an attempt is made to show that hydrogen discharged at the tip of the crack is responsible for crack propagation both in aqueous and organic media and that the failure is a highly specialised form of slow strain-rate embrittlement to which titanium alloys are susceptible when they contain intermediate amounts of hydrogen (Ti-5Al-2·5Sn, 250-750 ppm H) [7].

Experimental methods

The materials employed were commercially pure titanium (0·08%Fe, 30 ppm H) and Ti-5Al-2·5Sn (5·14%Al, 2·54%Sn, 0·07%Fe, 100 ppm H) in the form of annealed sheet, 0·025 in thick.

Two types of stress corrosion test were used: simple U-bend tests and dynamic tensile tests on an Instron tensile testing machine using notched and unnotched specimens in contact with the environment.

The tests were carried out in two environments: (a) aqueous chloride solutions ranging from distilled water (0·1 ppm Cl^-) to 3% NaCl (18000 ppm Cl^-) and (b) methanol containing 1·5 wt% HCl.

Hydrogen charging was carried out by cathodically polarizing specimens in a solution of 0·03N H_2SO_4 containing sodium sulphate to increase the conductivity, using platinum anodes. Charging was carried out at a current density of 50 mA/cm² for periods of up to 20 days.

Thermal hydrogen charging was employed to introduce controlled amounts of hydrogen in to the lattice. This was achieved by bleeding the required volume of hydrogen into a furnace at 600°C, followed by quenching.

The fracture surfaces obtained were examined by optical and scanning electron microscopy.

Experimental results

(a) *Aqueous chloride solutions*

Stress corrosion cracking in aqueous chloride solutions was observed in the Ti-5Al-2·5Sn alloy but not in the metal, which suffered dimple failure at all strain rates. Cracking in the Instron tests was indicated (i) by a considerable reduction in the total strain to failure, (ii) by failure without necking, a single crack occurring perpendicular to the fracture surface from the ductile dimple mode obtained in air (Fig. 1) to a transgranular cleavage mode, as shown in Fig. 2.

Cracking occurred very close to the U.T.S. over a narrow range of crosshead speeds, 0·005-0·05 cm/min for notched specimens and 0·05-0·2 cm/min for unnotched specimens.

(b) *Methanolic solutions*

The alloy exhibited stress corrosion cracking both in Instron tests at slow crosshead speeds ($\leqslant$0·05 cm/min) and in U-bend tests. These fracture surfaces were shown by scanning electron microscopy to consist of transgranular cleavage, with well-defined river patterns, as shown in Fig. 3.

The metal failed in U-bend tests after a longer period of immersion than the alloy, the fracture surface being intergranular. No cracking of the metal was observed in Instron tests.

This type of intergranular failure was also observed in unstressed specimens that were exposed over long periods of time and then broken in air. In the alloy, small areas of cleavage were occasionally observed in these fracture surfaces, as shown in Fig. 4, and in one specimen exposed for 35 days very severe embrittlement has occurred resulting in the unusual intergranular appearance shown in Fig. 5. Anodic polarisation at low current densities accelerated grain boundary attack and resulted in the selective removal of grains.

Hydrogen charging experiments

Cathodic polarization of stressed specimens of the alloy in 0·03N H_2SO_4, a solution employed by Tomashov [8], caused cracking after a period of 14 days at a current density of 50 mA/cm², using platinum anodes. The fracture surface produced was transgranular, showing poorly-defined cleavage, which may have been caused by hydride precipitation (Fig. 6). There was also evidence of etching and intergranular attack. Cracking did not occur in the metal under these conditions, but both materials exhibited extensive hydride precipitation when examined optically.

Since hydrogen is thought to be responsible for these phenomena, an attempt was made to simulate stress corrosion fracture surfaces by the addition of controlled amounts of hydrogen to the lattice. By completely saturating a specimen with hydrogen at 600°C, it became exceedingly

brittle. The fracture surface is shown in Fig. 7. In future work, it is hoped to show the effects of up to 1500 ppm hydrogen.

Discussion

The electrochemical conditions for cracking have been discussed in detail elsewhere [9,10]. The passive film must be broken in order to initiate corrosion attack. In many stress corrosion systems, crack initiation occurs at the yield point (or 0·1% Proof Stress) in dynamic straining experiments. This is to be expected since anodic dissolution will occur as pile-ups of dislocations fracture the passive film. The initiation of cracking close to the UTS in the alloy may be associated with the strain required to precipitate the hydride phase. This phase is formed rapidly when the alloy is heavily strained in a medium in which it suffers from stress corrosion cracking [11].

The proposed model of the crack propagation mechanism under stress corrosion conditions is one of successive hydride formation. Initially, the passive film is broken by an avalanche of dislocations cutting the surface, or, under crevice conditions, by a chemical breakdown of the film. In the first case, the delay in the repassivation of emergent slip steps will allow sufficient hydrogen to enter the lattice locally, and, aided by the dislocation movement, the hydride phase will form. The Ti-5Al-2·5Sn alloy exhibits co-planar arrays of dislocations [12] and will deform by coarse slip at low tensile strain producing wide slip steps which do not repassivate [9] as readily as fine slip steps. In the second case, the breakdown of passivity will produce the hydride phase since this always occurs whenever titanium is active [13].

The hydride phase forms on two of the three principle slip planes in the titanium lattice [14] and its formation will block the movement of dislocations in these planes. In the Ti-5Al-2·5Sn alloy, it can be inferred from the co-planarity of the dislocation arrays that cross-slip is difficult. This will result in a high rate of hardening along the slip planes. It is suggested that it is this hardening effect of the hydride phase that results in the cleavage clearly evident in Figs. 2 and 3. Blackburn [15] has shown that the cleavage plane in α-alloys under stress corrosion conditions is 14-16° from the basal plane. He has identified it as $(10\bar{1}7)$ or $(10\bar{1}8)$ and found that the same cleavage plane is also observed in air fractures. The failure of the titanium metal to suffer cracking in the H_2SO_4 charging experiments despite the presence of hydrides may be due to the easier climb of dislocations in the metal which reduces the maximum stress attainable at the end of a hydride precipitate.

The diffusion rate of the hydrogen atom in the α-titanium lattice is lower than the velocity of stress corrosion crack propagation. This difference must be accounted for, otherwise the role of hydrogen cannot be fully ex-

plained. The diffusion coefficient of hydrogen in α-titanium is $1{\cdot}1 \times 10^{-10}$ cm²/sec at room temperature [16]. The crack velocity (which varies considerably) for Ti-5Al-2·5Sn alloy in 3% NaCl solution is 0·9 cm/min. In 1 second a hydrogen atom will travel $1{\cdot}5 \times 10^{-5}$ cm, whereas the crack will have propagated $1{\cdot}5 \times 10^{-2}$ cm. Even allowing for the possibility that the plastic deformation at the tip of the crack may enhance the diffusion rate of hydrogen by some unknown amount the fracture will clearly be different from that observed by Williams [7] in Ti-5Al-2·5Sn alloy containing sufficient hydrogen to produce hydride by plastic deformation along the whole path of the fracture. There are two possibilities: (i) that the initiation of the hydride phase at the tip of the crack results in a complete fault along the whole of the slip plane in a single grain, producing a face-centred cubic phase which is not full of hydrogen but produces the same hardening effect, and (ii) that a small amount of hydride precipitate can cause cleavage over much greater distances than the length of the precipitate. Until more experimental evidence is obtained, either possibility may apply.

The strain rate $\dot{\epsilon}$ ahead of a crack propagating in the y direction is related to the crack velocity V in the following way [17]:

$$V = \frac{\partial y}{\partial t} = \frac{\dot{\epsilon}}{\partial \epsilon / \partial y}$$

Under the open circuit conditions of the Instron tests, $V = 0{\cdot}9$ cm/min. The strain gradient is unknown but is 1-15 cm^{-1} in steel and aluminium alloys [17]. Taking the lower value since the conditions were nearer to plane stress than plane strain, the strain rate ahead of a stress corrosion crack in the Ti-5Al-2·5Sn alloy is estimated to be 0·9 per minute. The range of strain rates that have been found to give strain induced hydrides is 10^{-3}-1 per minute.

Whether the amount of hydrogen being discharged at the tip of the crack is sufficient is difficult to calculate unless the amount of hydride produced is known. Tiner [18] has employed micro-antoradiography and shown that stress corrosion fracture surfaces in Ti-5Al-2·5Sn alloy exhibit hydrogen-free clevage areas and very small adjacent regions which contain hydrogen. Quantities cannot be estimated in this way although the analysis conforms to the fracture mechanism suggested above.

There is much evidence in the literature to support the hydrogen embrittlement theory. Since it is postulated that some critical amount of hydrogen in the lattice is required, an alloy with a high residual hydrogen content is more likely to be susceptible to cracking than one with a low hydrogen content. Sandoz and Newbegin [19] for example, have shown that the stress intensity factor (K) for a Ti-8Al-1Mo-IV alloy in air is lowered

near to the value required for stress corrosion as the dissolved hydrogen content is raised. Howe and Goode [20] have shown that vacuum annealing Ti-Al-Mo-V alloys considerably lowers the interstitial hydrogen content and eliminates stress corrosion susceptibility.

The slow loss of strength experienced by both materials in methanolic environments in the absence of stress is the result of preferential dissolution. Under open circuit conditions, hydrogen evolution will also occur. Certainly the cleavage regions seen in such fractures (Fig. 4) and the excessively embrittled fracture surface seen in Fig. 5 are probably the result of hydrogen adsorption, possibly also accompanied by dissolution.

References

1. LYON, R. N. *Liquid Metals Handbook*, Atomic Energy Commission, Washington, D.C., 1952.
2. KIEFFER, G. C. & HARPLE, W. W. *Met. Prog.*, vol. 63, p. 74, 1953.
3. BROWN, B. F. & BEACHEM, C. D. *Corr. Sci.*, vol. 5, p. 745, 1965.
4. PELLINI, W. S., GOODE, R. J. PUZAK, P. P., LANGE, E. A. & HUBER, R. W. U.S. NRL Report No. 6300, p. 62.
5. CURTIS, R. E. & SPURR, W. F. *Trans. A.S.M.*, vol. 61, p. 115, 1968.
6. BECK, T. R. *J. Electrochem. Soc.*, vol. 114, p. 551, 1967.
7. WILLIAMS, D. N. *J. Inst. Metals*, vol. 91, p. 147, 1962-3.
8. TOMASHOV, N. D. & MODESTOVA, V. N. *Corrosion of Metals and Alloys*, (trans. A. D. Mercer, ed. C. J. L. Booker), National Lending Library for Science and technology (Boston Spa, Yorkshire), p. 216, 1964.
9. SCULLY, J. C. *Corr. Sci.*, vol. 7, p. 197, 1967.
10. SCULLY, J. C. *Corr. Sci.*, in press.
11. SANDERSON, G. & SCULLY, J. C. *Corr. Sci.*, vol. 6, p. 541, 1966.
12. SANDERSON, G. & SCULLY, J. C. *Environmental-Sensitive Mechanical Behaviour* (ed. A. R. C. Westwood and N. S. Stoloff), Gordon and Breach (New York), p. 511, 1966.
13. OTSUKA, R. *Inst. Phys. and Chem. Res.*, Japan, vol. 54, p. 97, 1960.
14. SANDERSON, G. & SCULLY, J. C. *Trans. AIME Met. Soc.*, vol. 239, p. 1883, 1967.
15. BLACKBURN, M. J. *Fundamental Aspects of Stress Corrosion Cracking*, (ed. R. W. Staehle), Plenum Press (New York), to be published.
16. WASILEWSKI, R. J. & KEHL, G. L. *Metallurgia*, vol. 50, p. 225, 1954.
17. KANNINEN, M. K., MUKHERJEE, A. K., ROSENFIELD, A. R. & HAHN, G. T. *Symposium on Mechanical Behaviour of Materials under Dynamic Loads*, San Antonio, Texas, Sept., 1967.
18. TINER, N. A. Private communication, April, 1967.
19. SANDOZ, G., U.S. Naval Research Lab., Washington, D.C., Private communication, December, 1967.
20. HOWE, D. G. & GOODE, R. J., U.S. Naval Research Lab., Washington, D.C., private communication, December, 1967.

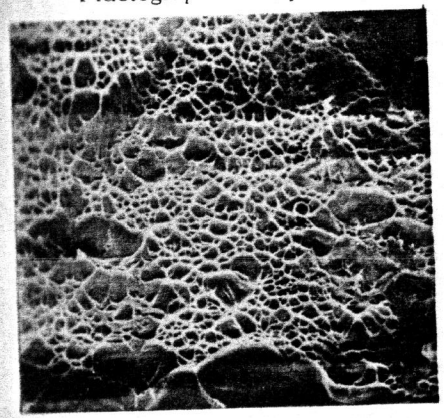

Fig. 1. Scanning electron micrograph illustrating the ductile dimple mode of fracture in the Ti-5Al-2·5Sn alloy. (Magnification 380 ×.)

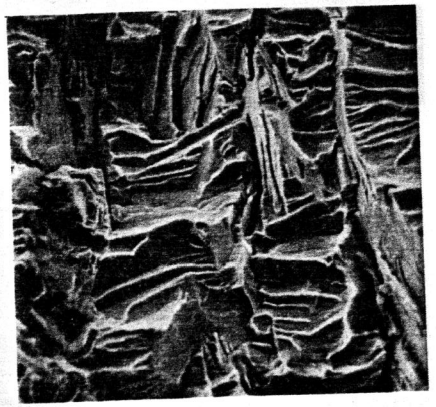

Fig. 2. Scanning electron micrograph of the fracture surface of a notched specimen of Ti-5Al-2·5Sn alloy pulled in 3% NaCl at a crosshead speed of 0·005 cm/min. (Magnification 430 ×.)

Fig. 3. Scanning electron micrograph of the fracture surface of a U-bend specimen of Ti-5Al-2·5Sn alloy cracked in MeOH/HCl. (Magnification 1120 ×.)

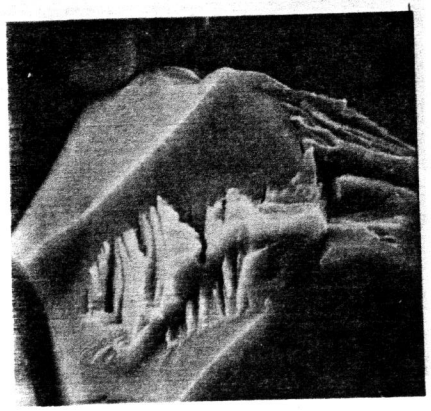

Fig. 4. Scanning electron micrograph of the fracture surface of a specimen of Ti-5Al-2·5Sn alloy pulled in air after immersion in MeOH/HCl. (Magnification 2250 ×.)

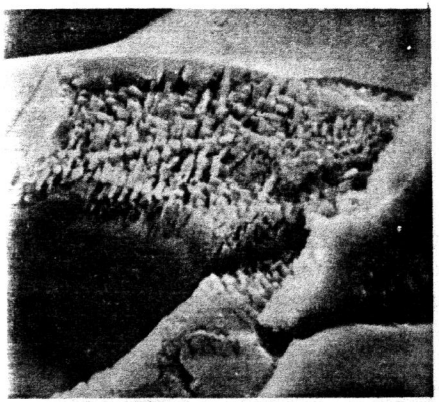

Fig. 5. Scanning electron micrograph of the fracture surface of a specimen of Ti-5Al-2·5Sn alloy severely embrittled by immersion in MeOH/HCl. (Magnification 2350 ×.)

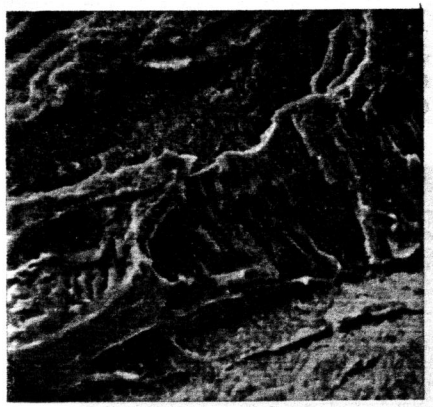

Fig. 6. Scanning electron micrograph of the fracture surface of a specimen of Ti-5Al-2·5Sn alloy cracked by charging in a solution of 0·03N H_2SO_4 at 50 mA/cm^2 for 14 days. (Magnification 710 ×.)

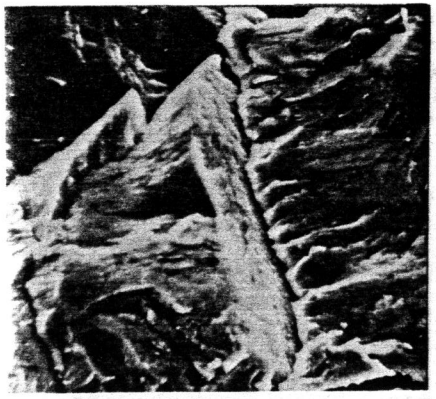

Fig. 7. Scanning electron micrograph of the fracture surface of a specimen of Ti-Al-2·5Sn alloy after severe embrittlement by charging with hydrogen at 600°C. (Magnification 1250 ×.)